DOA Estimation for Time-Modulated Linear Array Based on Golay-Paired Hadamard Matrix

Xinyi Zhou, Zihao Teng, *Graduate Student Member, IEEE*, Jiancheng An, *Senior Member, IEEE*, and Lu Gan, *Member, IEEE*

***Abstract*—This paper proposes a novel method for estimating the direction of arrival (DOA) in a time-modulated linear array (TMLA) based on the Golay-paired Hadamard (GPH) matrix. The objective is to address challenges presented by conventional TMLAs of limitations in the directional range due to the energy dispersion of radiation. To tackle this challenge, we construct a complete complementary set through the recursive derivation of the GPH matrix. From this set, we select mutually paired sequences that maintain an equal number of activated radio frequency switches, thereby designing an optimized time-modulated sequence. Theoretical analysis demonstrates that the proposed method can form an approximately flat sum beam across the entire spatial domain, thus facilitating an expansion of the directional measurement range. Furthermore, the DOA estimation is utilized by the multiple signal classification (MUSIC) algorithm. Simulation results validate the effectiveness of the proposed method. Specifically, the root mean square error is reduced by about 2.5° in the case of SNR of -10 dB.**

***Index Terms*—Golay-paired Hadamard (GPH) matrix, time-modulated linear array, direction of arrival (DOA), MUSIC algorithm.**

I. Introduction

With the rapid advancement of wireless transmission technology, the demands on high-performance antenna array systems in radar and communication systems have increased significantly, necessitating features such as low sidelobes [1], [2], high gain [3], [4], and accurate beamforming [5], [6]. Achieving these functionalities requires precise control over the amplitude and phase of each element, resulting in complex feed networks that substantially increase antenna costs. To address these challenges, the parameter time has been introduced as a novel dimension in array design. One prominent example of this concept is the time-modulated linear arrays (TMLA), which utilize the periodic switching of antenna elements to achieve dynamic radiation pattern control. By modulating the operational time of antenna elements, TMLA sequentially activates different elements at different time slots, enabling dynamic radiation pattern control without requiring simultaneous excitation of all elements, thereby simplifying the antenna feed network.

In particular, Shanks et al. leveraged the time domain as an additional variable to control antenna radiation characteristics [7], achieved through the periodic modulation of an antenna array's radiation pattern using radio frequency (RF) switches. Although subsequent research led to advancements such as rapid beam electronic scanning [8], ultra-low sidelobe beam pattern synthesis [9], and time-modulated phase center shifting [10], they relied on numerical simulations due to practical challenges, such as the limited switching speed of RF switches and sidelobe radiation interference. More recently, research has moved beyond theoretical analysis and numerical simulations to investigate various practical characteristics of time-modulated arrays, including directionality coefficients and gain [11], mutual coupling [12], and full-wave analysis [13]. Furthermore, the authors [14] investigated three-time modulation methods, namely variable aperture sizes (VAS), unidirectional phase center motion (UPCM), and bidirectional phase center motion (BPCM), examining their feeder dynamic ranges and sidelobe electrical characteristics. Building on these advancements, the research on time-modulated arrays has primarily focused on synthesizing ultra-low sidelobe patterns [15], suppressing sidelobe levels or radiated power [16][17], and beamforming [18]. Furthermore, the direction of arrival (DOA) estimation is a key technique in antenna systems that determines the direction from which signals arrive [19], [20], [21]. In [22], the UPCM approach was employed to integrate the multiple signal classification (MUSIC) algorithm with TMLA-based DOA estimation. Specifically, by harnessing the harmonic signals generated through time modulation, a multidimensional data space is constructed, thereby enhancing angular resolution and estimation accuracy. However, the UPCM scheme is limited by the design of time-modulated sequences, leading to notches in the antenna radiation pattern that reduce the angular range for DOA estimation.

Golay complementary sequences, known for their favorable autocorrelation and cross-correlation properties, are widely applied in signal processing and communications [23], [24], [25], [26]. The Golay-paired Hadamard (GPH) matrix extends this concept by constructing mutually orthogonal arrays of Golay complementary pairs [27], where each set contains complementary sequences that are mutually orthogonal. Inspired by the favorable properties of the GPH matrix, in this paper, we employ the GPH matrix to enhance the accuracy and directional coverage of DOA estimation by mitigating beam notches in antenna

Received 17 September 2025; accepted 31 October 2025. Date of publication 6 November 2025; date of current version 17 December 2025. This work was supported by the National Natural Science Foundation of China under Grant 62471096. The associate editor coordinating the review of this article and approving it for publication was Prof. Fangqing Wen. *(Corresponding author: Zihao Teng.)*

Xinyi Zhou and Lu Gan are with the School of Information and Communication Engineering, University of Electronic Science and Technology of China (UESTC), Chengdu 611731, China, and also with the Yibin Institute of UESTC, Yibin, 643000, China (e-mail: zhouxinyi@std.uestc.edu.cn; ganlu@uestc.edu.cn).

Zihao Teng is with the School of Information and Communication Engineering, University of Electronic Science and Technology of China (UESTC), Chengdu 611731, China (e-mail: tzhuestc@163.com).

Jiancheng An is with the School of Electrical and Electronics Engineering, Nanyang Technological University (NTU), Singapore 639798 (e-mail: jiancheng.an@ntu.edu.sg).

Digital Object Identifier 10.1109/LSP.2025.3629562

radiation patterns. Simulation results demonstrate the effectiveness of the proposed approach in substantially improving the accuracy and angular coverage of DOA estimation compared to conventional time modulation sequences.

II. System Model

Consider an N-element uniform linear array (ULA) composed of isotropic radiators with an inter-element spacing $d = \lambda/2$, where λ is the wavelength at the center operating frequency f_0. Each element is connected to a high-speed RF switch governed by a periodic time-modulation sequence of the element. The array factor of the TMLA is given by $F(\theta,t) = e^{j2\pi f_0 t}\sum_{k=1}^{N} I_k e^{j\alpha_k} U_k(t) e^{j(k-1)\beta d\sin\theta}$, where I_k and α_k are the static excitation amplitude and phase of the k-th oscillator, the static excitation parameters are set as $I_k = 1$ and $\alpha_k = 0, \forall k$. $\beta = \frac{2\pi f_0}{c}$, c is the speed of light in free space, θ denotes the azimuthal angle, and $U_k(t)(t \geq 0)$ denotes the switching function of the k-th oscillator,

$$U_k(t) = \sum_{m=1}^{N_c}\sum_{i=1}^{N} \boldsymbol{O}(k,i)\mathrm{rect}\left(\frac{t-(i-1)\tau-(m-1)T_p}{\tau}\right), \tag{1}$$

where T_p is the modulation period, $\tau = \frac{T_p}{N}$, $\boldsymbol{O}$ is the time modulation sequence, and $\boldsymbol{O}(k,i)$ denotes the (k,i)-th entry of $\boldsymbol{O}$, N_c is the total number of cycles, and $\mathrm{rect}(t) = \begin{cases} 1 & \text{for } 0 \leq t \leq 1 \\ 0 & \text{for } others \end{cases}$, denotes the rectangular window function. Due to the periodicity of $U_k(t)$, it can be decomposed into Fourier series, and the Fourier coefficients $b_{m,k}$ are

$$b_{m,k} = \frac{1}{T_p}\int_0^{T_p} U_k(t) e^{-j2\pi m f_p t} dt, \tag{2}$$

where $f_p = \frac{1}{T_p}$ is the modulation frequency.

Assume that L far-field narrowband signals with directions of arrival $\theta_1, \theta_2, \ldots, \theta_L$ incident into an N-element TMLA, and all signals share the same carrier frequency f_0. After the temporal modulation by the RF switches, the signals are Fourier-expanded to obtain the m-th order sideband signal at the corresponding frequency $f_0 + mf_p, m = 0, \pm1, \pm2, \ldots, \pm\infty$. The m-th sideband signal can be expressed as

$$x_m(t) = \sum_{l=1}^{L}\sum_{k=1}^{N} b_{m,k}\left[s_l(t)e^{j2\pi m f_p t}e^{j(k-1)\beta d\sin\theta_l} + n_k(t)\right], \tag{3}$$

where $s_l(t)$ is the l-th far-field signal with incidence angle θ_l, and $n_k(t)$ denotes the additive white Gaussian noise (AWGN) with zero mean and variance σ^2. In the formulation, both the desired signal and $n_k(t)$ are subject to the same time-modulation process, since the noise originates at the antenna element level, primarily from receiver front-end components such as the low-noise amplifier and RF switch, and is therefore inherently synchronized with the time-modulated signal path. After that, all the sideband signals are mixed and filtered. To separate the different sideband signals, it is necessary to down-convert the signal to the same intermediate frequency (IF) stage. The resulting output signal $y_m(t)$ is expressed as

$$y_m(t) = \sum_{l=1}^{L}\sum_{k=1}^{N} b_{m,k}\left[s_l^{IF}(t)e^{j(k-1)\beta d\sin\theta_l} + n_k(t)\right], \tag{4}$$

where $s_l^{IF}(t)$ denotes the IF signal of $s_l(t)$. Let Q be the maximum order of the sideband. By collecting all sideband signals, the output signal can be rewritten in matrix form

$$\boldsymbol{y}(n) = \boldsymbol{B}^T\left[\boldsymbol{A}\boldsymbol{s}(n) + \boldsymbol{z}(n)\right], (n = 1, 2, \ldots, N_s), \tag{5}$$

where N_s is the number of available snapshots,

$$\begin{aligned}
\boldsymbol{y}(n) &= [y_{-Q}(n), y_{-Q+1}(n), \ldots, y_Q(n)]^T \in \mathbb{C}^{2Q+1}, \\
\boldsymbol{s}(n) &= [s_1^{IF}(n), s_2^{IF}(n), \ldots, s_L^{IF}(n)]^T \in \mathbb{C}^L, \\
\boldsymbol{z}(n) &= [n_1(n), n_2(n), \ldots, n_N(n)]^T \in \mathbb{C}^N, \\
\boldsymbol{A} &= [\boldsymbol{a}(\theta_1), \boldsymbol{a}(\theta_2), \ldots, \boldsymbol{a}(\theta_L)] \in \mathbb{C}^{N\times L}, \\
\boldsymbol{a}(\theta_l) &= [1, e^{j\beta d\sin\theta_l}, \ldots, e^{j(N-1)\beta d\sin\theta_l}]^T \in \mathbb{C}^N
\end{aligned}$$

, and the matrix $\boldsymbol{B}$ can be expressed as:

$$\boldsymbol{B} = \begin{bmatrix} b_{-Q,1} & b_{-Q+1,1} & \cdots & b_{Q,1} \\ b_{-Q,2} & b_{-Q+1,2} & \cdots & b_{Q,2} \\ \vdots & \vdots & \ddots & \vdots \\ b_{-Q,N} & b_{-Q+1,N} & \cdots & b_{Q,N} \end{bmatrix} \in \mathbb{C}^{N\times(2Q+1)}. \tag{6}$$

III. DOA Estimation Using GPH Scheme

To design the time modulation sequences for enhancing DOA estimation, we first introduce the concept of Golay complementary sequences and discuss their fundamental properties. Based on this, the construction method of GPH matrices is presented. Finally, we design the time modulation sequences for the TMLA by leveraging the GPH matrix.

A. Golay Complementary Sequences

For any two sequences $\boldsymbol{a} = [a_0, a_1, \ldots, a_{N-1}]^T$ and $\boldsymbol{b} = [b_0, b_1, \ldots, b_{N-1}]^T$ of length N, $\forall i$, a_i, $b_i \in \{-1, 1\}$. The sequences $\boldsymbol{a}$ and $\boldsymbol{b}$ are defined as a pair of Golay complementary sequences if they satisfy the condition

$$G_{\boldsymbol{a}}(k) + G_{\boldsymbol{b}}(k) = \begin{cases} 0 & \text{for } k \neq 0 \\ 2N & \text{for } k = 0 \end{cases},$$

where $G_{\boldsymbol{a}}(k) = \sum_{m=0}^{N-1-k} a_m a_{m+k}$ denotes the autocorrelation function of sequence $\boldsymbol{a}$. Let $A_m = \sum_{n=1}^{N} a_n e^{-j2\pi m\frac{n}{N}}$, $B_m = \sum_{n=1}^{N} b_n e^{-j2\pi m\frac{n}{N}}$ denote the Fourier coefficients of $\boldsymbol{a}$ and $\boldsymbol{b}$, then we have [24]

$$|A_m|^2 + |B_m|^2 = 2N. \tag{7}$$

B. GPH Matrix Construction Method

GPH matrices are obtained by uniformly randomly selecting M rows in an $N \times N$ matrix $\boldsymbol{P}_N = \boldsymbol{H}\boldsymbol{G}$, where $\boldsymbol{H}$ is a Walsh-Hadamard transform (WHT) matrix [28], and $\boldsymbol{G}$ is a diagonal matrix whose diagonal elements are sequences from a Golay complementary pair. Given an $N \times N$ GPH matrix $\boldsymbol{P}_N$, the GPH matrix $\boldsymbol{P}_{2^{\sim}N}$ of dimension $2^{\sim}N \times 2N$ can be generated by $\boldsymbol{P}_{2^{\sim}N} = [\boldsymbol{P}_N, \tilde{\boldsymbol{P}}_N; \boldsymbol{P}_N, -\tilde{\boldsymbol{P}}_N]$, where $\tilde{\boldsymbol{P}}_N = \boldsymbol{E}_N\boldsymbol{P}_N$ denotes the equivalent Hadamard matrix obtained by permuting the rows and columns of $\boldsymbol{P}_N$. $\boldsymbol{E}_N = [\boldsymbol{0}, \boldsymbol{I}_{N/2}; \boldsymbol{I}_{N/2}, \boldsymbol{0}]$, where $\boldsymbol{I}_{N/2}$ is a unit matrix of order $N/2$. The matrix $\boldsymbol{P}_{2^{\sim}N}$ constructed by this method guarantees orthogonality between rows and columns. Moreover, it can be observed that the matrix $\tilde{\boldsymbol{P}}_N$ can be obtained by exchanging the upper and lower halves of $\boldsymbol{P}_N$, which results in excellent complementary properties [27].

C. Principle of DOA Estimation With GPH Scheme

In the previous section, we examined the construction and associated properties of the GPH matrix. Subsequently, we

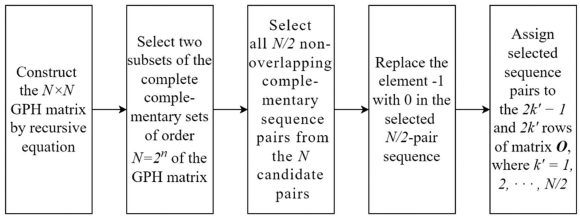

Fig. 1. Flowchart for the design of the time modulation matrix for the TMLA with GPH scheme.

will delve into its application in designing time-modulating sequences, followed by the estimation of DOA based on the given time-modulation sequences.

Considering an array with $N = 2^n$ antennas[1] and the N-order entirely complementary set can be obtained by recursively deriving the GPH matrix. To optimize the sequence selection while avoiding redundancy, we implement a systematic selection strategy as follows. First of all, we select all $N/2$ non-overlapping complementary sequence pairs from N candidate pairs, noting from the definition of the GPH matrix [27]. We construct matrix $\boldsymbol{O}$ using these $N/2$ complementary sequence pairs. Each Golay complementary pair forms a consecutive row pair in matrix $\boldsymbol{O}$, namely the $2^{\sim}k' - 1$-th and $2^{\sim}k'$-th rows for $k' = 1, 2, \ldots, N/2$, resulting in a total of N rows in the matrix. In addition, we use '1's and '0's to denote the 'on' and 'off' states of the RF switch in TMA, however, the elements in the original Golay complementary sequence are ± 1, so we replace -1 with 0 in the matrix $\boldsymbol{O}$. Fig. 1 illustrates the flowchart of designing the time modulation matrix $\boldsymbol{O}$ for the TMLA with the GPH scheme.

After constructing the matrix $\boldsymbol{O}$, the time modulation function $U_k(t)$ can be known from (1). The DOAs of signals are estimated by MUSIC spatial spectral peak search [22].

D. Performance Analysis

In this subsection, the effectiveness of the proposed method is evaluated using the total antenna radiated power $P(\theta)$, which can be obtained as

$$P(\theta) = \sum_{m=-Q}^{Q} \left| \sum_{k=1}^{N} b_{m,k} e^{j(k-1)\beta d \sin\theta} \right|^2 = \sum_{m=-Q}^{Q} \left[\sum_{k=1}^{N} |b_{m,k}|^2 + \sum_{n\neq k} b_{m,k} b_{m,n}^* e^{-j\beta d sin\theta (k-n)} \right]. \tag{8}$$

To calculate (8), we firstly calculate each $b_{m,k}$ by substituting (1) into (2). Since $U_k(t)$ is periodic, we start by taking one periodic for the calculation

$$b_{m,k} = \frac{1}{T_p} \int_0^{T_p} \sum_{i=1}^{N} \boldsymbol{O}(k,i) \text{rect}\left[\frac{t-(i-1)\tau}{\tau}\right] e^{-j2\pi m f_p t} dt = \frac{1}{N} \text{sinc}\left(\frac{m}{N}\right) \cdot e^{j\pi \frac{m}{N}} \sum_{i=1}^{N} \boldsymbol{O}(k,i) \cdot e^{-j2\pi m \frac{i}{N}}. \tag{9}$$

[1]When the number of antennas does not satisfy $N = 2^n$, we adopt the minimum redundancy array (MRA) [29] design criterion for selecting $2^{\lfloor \log_2(N) \rfloor}$ elements.

Let $S_{m,k} = \sum_{i=1}^{N} \boldsymbol{O}(k,i) \cdot e^{-j2\pi m \frac{i}{N}}$, then

$$b_{m,k} = \frac{1}{N} \text{sinc}\left(\frac{m}{N}\right) \cdot e^{j\pi \frac{m}{N}} \cdot S_{m,k}. \tag{10}$$

Let $\boldsymbol{P}_o$ denotes the matrix consisting of the original Golay's complement sequence corresponding to matrix $\boldsymbol{O}$, since the value -1 in the original Golay complementary sequences is replaced with 0 to design the switching sequences, we have $\boldsymbol{O}(k,i) = \frac{\boldsymbol{P}_o(k,i)+1}{2}$. Notice that $\sum_{i=1}^{N} e^{-j2\pi m \frac{i}{N}} = 0 (m \neq 0)$, thus the sequence satisfies $S_{m,k} = \sum_{i=1}^{N} \frac{\boldsymbol{P}_o(k,i)+1}{2} e^{-j2\pi m \frac{i}{N}} = \frac{1}{2} X_k$, where $X_k = \sum_{i=1}^{N} \boldsymbol{P}_o(k,i) \cdot e^{-j2\pi m \frac{i}{N}}$ is the Fourier coefficients of the matrix $\boldsymbol{P}_o$. Since rows $2^{\sim}k' - 1$ and $2^{\sim}k' (k' = 1, 2, \ldots, \frac{N}{2})$ in the time modulation matrix $\boldsymbol{O}$ is a pair of Golay complementary sequences, then from (7), we have

$$|S_{m,2k'-1}|^2 + |S_{m,2k'}|^2 = \frac{1}{4}\left(|X_{2k'-1}|^2 + |X_{2k'}|^2\right) = \frac{N}{2}. \tag{11}$$

Substituting (11) into (10) yields

$$|b_{m,2k'-1}|^2 + |b_{m,2k'}|^2 = \frac{1}{2N} \text{sinc}^2\left(\frac{m}{N}\right). \tag{12}$$

Substituting (12) into (8) yields

$$\begin{aligned} P(\theta) &= \sum_{m=-Q}^{Q} \left[\frac{1}{4} \text{sinc}^2\left(\frac{m}{N}\right) + \sum_{n\neq k} b_{m,k} b_{m,n}^* e^{-j(k-n)\beta d \sin\theta} \right] \\ &= \sum_{m=-Q}^{Q} \left[\frac{1}{4} \text{sinc}^2\left(\frac{m}{N}\right) + \frac{1}{N^2} \cdot \sum_{n\neq k} \sum_{i=1}^{N} \text{sinc}^2\left(\frac{m}{N}\right) \boldsymbol{O}(k,i) \boldsymbol{O}(n,i) \cdot e^{-j(k-n)\beta d \sin\theta} \right]. \end{aligned} \tag{13}$$

Since the value of the $\frac{1}{N^2}$ becomes progressively smaller as N increases, thus

$$P(\theta) \approx \sum_{m=-Q}^{Q} \left[\frac{1}{4} \text{sinc}^2\left(\frac{m}{N}\right) \right]. \tag{14}$$

From (14), it is apparent that $P(\theta)$ is irrelevant to θ, the favorable autocorrelation characteristics of the GPH matrix enable the harmonic energy in non-mainlobe directions to cancel each other out effectively, thus form an approximately flat sum beam across the entire spatial domain.

IV. Simulation Results

In this section, we assess the directional range and accuracy of the DOA estimation method utilizing the GPH matrix scheme within the TMLA. We consider an 8-element TMLA with isotropic elements and a half-wavelength uniform spacing. The DOA estimation is employed by the MUSIC algorithm [22]. All statistical results were conducted based on 1,000 independent Monte Carlo trials.

A. Patterns of TMLA With the Proposed Method

In this subsection, the performance of the proposed method is evaluated through the beam pattern. The corresponding antenna radiation pattern at frequency $f_0 + mf_p (m = 0, \pm 1, \pm 2)$ is illustrated in Fig. 2. It is observed that the main lobe is consistently directed at 0°, with a sidelobe level (SLL) of 12.38 dB. Additionally, the patterns of the $\pm m (m \neq 0)$-th order side lobes

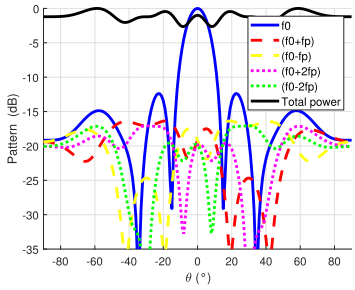

Fig. 2. Patterns in 8-element TMLA with GPH scheme and total power beam pattern.

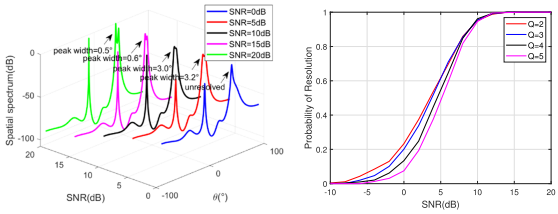

(a) (b)

Fig. 3. (a) Spatial spectrum versus SNR; (b) Probability of resolution versus SNR with different Q.

exhibit symmetry with respect to the normal axis of the TMLA. Furthermore, the total beam pattern, obtained by summing the sideband array factors, is presented. The energy in the harmonic directions cancels each other out, resulting in the total radiation power approaching a flat response.

B. Spatial Spectrum

Assume there are three far-field, narrowband, uncorrelated signals, each possessing equal power, the same carrier frequency f_0, and bandwidth, arriving from $-10°$, $40°$, and $45°$, respectively, with snapshots $N_s = 200$ and a sidelobe order $Q = 3$. Fig. 3(a) illustrates the relationship between the spatial spectrum and the signal-to-noise ratio (SNR). At SNR $= 5$ dB, the peak width at $\theta = 40°$ is $3.2°$, as SNR increases, the peak width decreases to $0.5°$. Notice that the two closely-spaced sources remain unresolved at SNR $= 0$ dB, and thus no peak width is annotated. It is evident that at low SNR levels, the resolution of the spatial spectrum is low, and the resolution performance gets better as the SNR increases, while the DOA of the three signals can be successfully determined by the location of the peaks in the spatial spectrum at high SNR levels.

Fig. 3(b) depicts the probability of successfully resolving two closely angles for different Q and illustrates the relationship between the DOA resolution performance and the sidelobe order. The parameters are set to $N_s = 200$, the signal are located as $35°$ and $40°$ and uncorrelated with each other. It can be observed that, for a given Q, the probility of successfully resolution increases with SNR and achieves 100% at SNR $= 16$ dB. However, the resolution degrades as Q increases. This because, although increasing Q theoretically expands the virtual aperture, it incorporates higher-order harmonics with low signal energy. These low-SNR components severely corrupt the sample covariance matrix, introducing bias and dispersion into the estimated noise subspace. Consequently, the orthogonality between the signal and noise subspaces is compromised, resulting in spectral broadening, spurious peaks, and ultimately, impaired resolution.

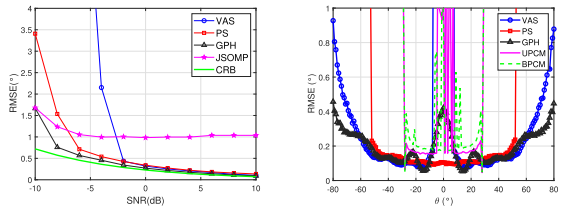

(a) (b)

Fig. 4. (a) RMSEs of the DOA estimation versus SNR; (b) RMSEs of the DOA estimation versus θ.

C. The Accuracy Performance

In this subsection, we evaluate the precision performance of DOA estimation under different parameters. The snapshot number is $N_s = 500$, and the DOAs of the three signals are $(-20°, 30°, 45°)$ Fig. 4(a) illustrates the sum root mean square error (RMSE) of traditional time modulation schemes such as VAS [14], pulse shifting (PS) [8], alongside the joint signal recovery and DOA estimation method (JSOMP) [30] and the proposed method under different SNR. It is evident that the RMSE of all schemes decreases as the SNR increases. Notably, compared with other modulation schemes, the proposed method has the lowest RMSE, especially when the SNR is low, and closely approaches the corresponding Cramér–Rao bound (CRB), demonstrating its effectivenes in practical scenarios.

Next, we evaluate the performance of DOA estimation for a single signal from $-85°$ to $85°$, with $Q = 3$ and a low SNR $= 0$ dB. For the UPCM [10] and BPCM [14] schemes, we set $M = 4$, where M denotes the number of elements that turn on for each time step τ, the RMSE of the DOA estimation is depicted in Fig. 4(b). It can be observed that BPCM and UPCM are only effective when the signal arrives from directions within $(-30°, 30°)$, as the RMSE exhibits spurious peaks at $\pm 30°$, adversely affecting the accuracy of the DOA estimation. Furthermore, BPCM exhibits slightly better estimation accuracy than UPCM. In contrast, the PS, VAS, and the proposed modulation scheme are able to maintain high estimation accuracy across the entire range from $-85°$ to $85°$. Although within the range of $(-10°, 10°)$, the estimation accuracy of BPCM and PS is marginally superior to that of the proposed method, it is essential to note that the proposed scheme's directional range is significantly broader than that of BPCM and UPCM. It can be observed that the estimation accuracies of VAS, UPCM, and BPCM in the range of $(-10°, 10°)$ deteriorate significantly, which verifies the stability of the proposed scheme at low SNR. Moreover, the RMSE of the proposed scheme is lower than that of the conventional time modulation scheme in most of the angular ranges.

V. Conclusion

In this paper, we employed the GPH matrix to enhance the performance of DOA estimation for TMLA. Specifically, by utilizing the orthogonality and complementarity intrinsic to the GPH matrix, we addressed the limitations associated with the DOA estimation range that arise from beam nulls in conventional TMLA antennas. Furthermore, theoretical analysis demonstrates the advantages conferred by sequence complementarity. Simulation experiments indicate that the proposed algorithm can achieve enhanced estimation accuracy and performance relative to traditional TMLAs.

REFERENCES

[1] H. Schrank, "Low sidelobe phased array antennas," *IEEE Antennas Propag. Soc. Newslett.*, vol. MAP-25, no. 2, pp. 4–9, Apr. 1983.

[2] Z. Teng et al., "Phased-array beampattern synthesis with a tradeoff between sparsity and sidelobe level," *Signal Process.*, vol. 214, 2024, Art. no. 109227.

[3] R. C. Mailloux, *Phased Array Antenna Handbook*, 2nd ed. Boston, MA, USA: Artech House, 2005.

[4] Z. Teng, H. Zhang, J. An, L. Gan, H. Li, and C. Yuen, "Low-complexity frequency invariant beamformer design based on SRV-constrained array response control," in *Proc. IEEE 99th Veh. Technol. Conf.*, 2024, pp. 1–5.

[5] S. X. Wu, A. M.-C. So, J. Pan, and W.-K. Ma, "Semidefinite relaxation and approximation analysis of a beamformed Alamouti scheme for relay beamforming networks," *IEEE Trans. Signal Process.*, vol. 65, no. 9, pp. 2428–2443, May 2017.

[6] Z. Teng, L. Gao, L. Gan, H. Liao, K. Du, and H. Jiang, "Accurate spatial-frequency response controllable frequency invariant beampattern synthesis with minimum beamwidth," *IEEE Trans. Antennas Propag.*, vol. 71, no. 7, pp. 6266–6271, Jul. 2023.

[7] H. Shanks and R. Bickmore, "Four-dimensional electromagnetic radiators," *Can. J. Phys.*, vol. 37, no. 3, pp. 263–275, 1959.

[8] H. Shanks, "A new technique for electronic scanning," *IRE Trans. Antennas Propag.*, vol. 9, no. 2, pp. 162–166, 1961.

[9] W. Kummer, A. Villeneuve, T. Fong, and F. Terrio, "Ultra-low sidelobes from time-modulated arrays," *IEEE Trans. Antennas Propag.*, vol. AP-11, no. 6, pp. 633–639, Nov. 1963.

[10] B. Lewis and J. Evins, "A new technique for reducing radar response to signals entering antenna sidelobes," *IEEE Trans. Antennas Propag.*, vol. AP-31, no. 6, pp. 993–996, Nov. 1983.

[11] S. Yang, Y. B. Gan, and P. K. Tan, "Evaluation of directivity and gain for time-modulated linear antenna arrays," *Microw. Opt. Technol. Lett.*, vol. 42, no. 2, pp. 167–171, 2004.

[12] S. Yang and Z. Nie, "Mutual coupling compensation in time modulated linear antenna arrays," *IEEE Trans. Antennas Propag.*, vol. 53, no. 12, pp. 4182–4185, Dec. 2005.

[13] X. Zhu, S. Yang, and Z. Nie, "Full-wave simulation of time modulated linear antenna arrays in frequency domain," *IEEE Trans. Antennas Propag.*, vol. 56, no. 5, pp. 1479–1482, May 2008.

[14] S. Yang, Y. Gan, and P. Tan, "Comparative study of low sidelobe time modulated linear arrays with different time schemes," *J. Electromagn. Waves Appl.*, vol. 18, no. 11, pp. 1443–1458, 2004.

[15] L. Zheng, S. Yang, Q. Zhu, and Z. Nie, "A projection-based approach for ultra-low side-lobe pattern synthesis in time-modulated spherical arrays," *Electromagnetics*, vol. 32, no. 2, pp. 61–76, 2012.

[16] Q. Chen, J.-D. Zhang, D.-Y. Luo, W. Wu, Y. Yu, and D.-G. Fang, "Low-sidelobe single-sideband time-modulated phased array using stepped waveforms with different amplitudes," *IEEE Trans. Antennas Propag.*, vol. 71, no. 12, pp. 9643–9654, Dec. 2023.

[17] C. He, H. Yu, X. Liang, J. Geng, and R. Jin, "Sideband radiation level suppression in time-modulated array by nonuniform period modulation," *IEEE Antennas Wireless Propag. Lett.*, vol. 14, pp. 606–609, 2015.

[18] S. K. Mandal, G. Mahanti, and G. Rowdra, "Synthesis of flat top beam pattern through time modulation of linear array," in *Proc. IEEE Conf. Signal Process. Commun. Comput.*, 2012, pp. 32–37.

[19] L. Liu, Z. Zhang, X. Zhang, P. Wei, J. An, and H. Li, "Joint spectrum sensing and DOA estimation based on a resource-efficient sub-Nyquist array receiver," *IEEE Trans. Signal Process.*, vol. 72, pp. 5354–5370, 2024.

[20] L. Liu, Z. Li, J. An, L. Gan, and H. Li, "DoA estimation for switch-element arrays based on sparse representation," in *Proc. IEEE Int. Conf. Acoust., Speech Signal Process.*, 2024, pp. 8506–8510.

[21] S. Lin, J. An, L. Gan, and M. Debbah, "UAV-mounted SIM: A hybrid optical-electronic neural network for DoA estimation," in *Proc. IEEE Int. Conf. Acoust., Speech Signal Process.*, 2025, pp. 1–5.

[22] G. Li, S. Yang, and Z. Nie, "Direction of arrival estimation in time modulated linear arrays with unidirectional phase center motion," *IEEE Trans. Antennas Propag.*, vol. 58, no. 4, pp. 1105–1111, Apr. 2010.

[23] F. Li, Y. Jiang, C. Du, and X. Wang, "Construction of Golay complementary matrices and its applications to MIMO omnidirectional transmission," *IEEE Trans. Signal Process.*, vol. 69, pp. 2100–2113, 2021.

[24] P. Ramezani, M. A. Girnyk, and E. Björnson, "On broad-beam reflection for dual-polarized RIS-assisted MIMO systems," *IEEE Trans. Wireless Commun.*, vol. 24, no. 2, pp. 1264–1277, Feb. 2025.

[25] C. De Marziani et al., "Modular architecture for efficient generation and correlation of complementary set of sequences," *IEEE Trans. Signal Process.*, vol. 55, no. 5, pp. 2323–2337, May 2007.

[26] Z.-J. Wu, C.-X. Wang, P.-H. Jiang, and Z.-Q. Zhou, "Range-doppler sidelobe suppression for pulsed radar based on Golay complementary codes," *Signal Process.*, vol. 27, pp. 1205–1209, 2020.

[27] X. Huang and Y. Li, "Scalable complete complementary sets of sequences," in *Proc. 2002 IEEE Glob. Telecommun. Conf.*, 2002, vol. 2, pp. 1056–1060.

[28] L. Gan, K. Li, and C. Ling, "Golay meets Hadamard: Golay-paired hadamard matrices for fast compressed sensing," in *Proc. 2012 IEEE Inf. Theory Workshop*, 2012, pp. 637–641.

[29] A. Moffet, "Minimum-redundancy linear arrays," *IEEE Trans. Antennas Propag.*, vol. AP-16, no. 2, pp. 172–175, Mar. 1968.

[30] L. Liu, Z. Li, J. An, L. Gan, and H. Li, "A CCM-based joint DOA-frequency estimation and signal recovery with efficient sub-Nyquist sampling," in *Proc. IEEE Int. Conf. Acoust., Speech Signal Process.*, 2024, pp. 8501–8505.